Available online at www.sciencedirect.com

ScienceDirect

Biomedical Journal

journal homepage: www.elsevier.com/locate/bj

Original Article

The effect of spatial resolution on the reproducibility of diffusion imaging when controlled signal to noise ratio

Yao-Liang Chen [a,b,1], Yu-Jen Lin [c,1], Sung-Han Lin [b], Chih-Chien Tsai [d], Yu-Chun Lin [b,e], Jur-Shan Cheng [f], Jiun-Jie Wang [a,b,d,*]

[a] Department of Diagnostic Radiology, Chang Gung Memorial Hospital at Keelung, Keelung, Taiwan
[b] Department of Medical Imaging and Radiological Sciences, Chang Gung University, Taoyuan, Taiwan
[c] Department of Radiation Oncology, Chang Gung Memorial Hospital at Linkou, Taoyuan, Taiwan
[d] Healthy Aging Research Center, Chang Gung University, Taoyuan, Taiwan
[e] Department of Medical Imaging and Intervention, Chang Gung Memorial Hospital at Linkou, Taoyuan, Taiwan
[f] Clinical Informatics and Medical Statistics Research Center, Chang Gung University, Taoyuan, Taiwan

ARTICLE INFO

Article history:
Received 14 September 2018
Accepted 11 March 2019
Available online 27 September 2019

Keywords:
Diffusion imaging
Reproducibility
Spatial resolution
2 compartment phantom

ABSTRACT

Background: The purpose of the study is to evaluate the reproducibility and repeatability of the compartmental diffusion measurement.

Methods: Two identical whipping cream phantoms and two healthy Sprague–Dawley rats were scanned on a 7T MR scanner, each repeated for three times. Diffusion weighted images were acquired along 30 non-collinear gradient directions, each with four b-values of 750, 1500, 2250 and 3000 s/mm^2. Slice thickness and field of view were used to create different combinations of voxel sizes, varied between 1.210 and 2.366 mm^3 in phantom and 0.200–0.303 mm^3 in rat brains. Multiple averages were used to achieve a controlled signal to noise ratio.

Results: Diffusion imaging showed good stability throughout the range of voxel sizes acquired from either the cream phantom or the rat, when the signal to noise ratio is controlled. The reproducibility analysis showed the within-subject coefficient of variation varied between 0.88% and 6.99% for phantom and 0.69%–6.19% for rat. Diffusion imaging is stable among different voxel sizes in 3 aspects: A. from both compartments in phantom and in the rat; B. in measurement of diffusivity and kurtosis and C. along axial, radial and averaged in all directions.

Conclusion: Diffusion imaging in a heterogeneous but isotropic phantom and *in vivo* is consistent within the range of spatial resolution in preclinical use and when the signal to noise ratio is fixed. The result is reproducible for repeated measurements.

* Corresponding author. Department of Medical Imaging and Radiological Sciences, Chang Gung University, 259 WenHua 1st Rd., Gueishan, Taoyuan 333, Taiwan.
E-mail address: jwang@mail.cgu.edu.tw (J.-J. Wang).
Peer review under responsibility of Chang Gung University.
[1] The first two authors contributed equally.
https://doi.org/10.1016/j.bj.2019.03.002
2319-4170/© 2019 Chang Gung University. Publishing services by Elsevier B.V. This is an open access article under the CC BY-NC-ND license (http://creativecommons.org/licenses/by-nc-nd/4.0/).

At a glance commentary

Scientific background on the subject

The water diffusion *in vivo* is deviated from Gaussianity because of hinderance and restriction from the cell membranes and organelles. The study investigated the effect of voxel size, which can be associated with the underlying microenvironment complexity, on the measurement of diffusion when inherent factor such as signal to noise ratio was fixed.

What this study adds to the field

The measurement of diffusion by using Magnetic Resonance Imaging in a heterogeneous but isotropic phantom and in the rat brain is consistent within the range of voxel size for preclinical use and under a fixed signal to noise ratio. The result is reproducible for repeated measurements.

Diffusion MRI has been widely used to investigate the change of tissue microstructure during a pathological process [1–4]. In order to characterize the directional dependence of water diffusion, diffusion tensor imaging was proposed [5,6], with many successes in studies of neurological diseases [7–9] and white matter fibers tractography [10,11]. The measurement of water diffusion by MRI often assumes that the diffusion occurs in a free and homogeneous environment [12]. However, compartmental diffusion might occur in the biological tissue because the cell membranes and organelles could act as barriers. As a result, the distribution of water diffusion could be deviated from the assumption of Gaussianity. Diffusion kurtosis imaging has been proposed to probe the non-gaussian nature of compartmental diffusion [13–15]. Both DTI and DKI could provide semi-quantitative parameters, such as the diffusivity and the diffusion kurtosis along either the radial or axial directions, or their averages (mean diffusivity and mean diffusion kurtosis).

The effect of signal to noise ratio on the diffusion measurement could be complicated in a compartmental model, because the signal decay is multi-exponential. The spatial resolution might further contribute to the variation of the measured diffusion parameters because the reduced voxel size is associated with decreased SNR [16]. The diffusion kurtosis in a two compartment model could be overestimated at reduced slice thickness up to 4 mm [17]. Unfortunately this very large voxel size could not be used in general preclinical routine because of poor anatomical information. These observation leads to concerns about the reproducibility and repeatability in a diffusion measurement because the comparison between studies might be invalid if the diffusion properties change significantly with the voxel sizes.

The whipping cream has been previously proposed as a good model for compartmental diffusion, because both the measured diffusion coefficient and mean kurtosis are similar to that in human brain [17]. The fat and water components in the cream phantom will be spatially separated by 3.5 ppm because of chemical shift effect, thus created a portion of single compartment diffusion, i.e. water as well as fat, and a portion of two-compartment diffusion, i.e. cream. This study proposed to investigate the dependence of diffusion measurement on spatial resolution in a range which is in current use for rat study while the SNR remained constant. Both the reproducibility and repeatability of diffusion measurements in a non-gaussian environment will be examined in a two-compartment phantom and in a biological environment *in vivo*.

Methods and materials

Preparation of phantom and rat

Whipping cream (35.1% fat, "Whipping Cream", President, manufactured by Societe Laitere de L'Hermitage, France) was filled into two 50 mL centrifuge tubes, which were placed in the scan room of a controlled room temperature (22 °C) for a prolonged period. Two phantoms were created, each was scanned three times in an interleaved manner.

The *in vivo* reproducibility was evaluated using two healthy rats (Sprague–Dawley, 300–400 g). Each rat was imaged three times separated by one week. All procedures were in accordance with and approved by the institution's Animal Care and Use Committee. A dedicated rat holder with both tooth and ear bars was used to fix the head of the animal. During the imaging experiment, the rat was anesthetized at 2–3% isoflurane and the temperature was maintained at 37 °C using circulating warm water. The heart rate, respiration and body temperature were monitored.

Images acquisition

A 7T MR scanner (ClinScan, Bruker BioSpin, Ettlingen, Germany) was used in the experiment. The phantom was allocated in the center of the magnetic field. Diffusion weighted images were acquired using a spin-echo echo planar imaging sequence with a mouse body coil. Thirty non-collinear diffusion weighted gradient directions were applied, which distributed over a full sphere optimized by the static electron repulsion model. For each gradient direction, 4 different b-values were used, including 750, 1500, 2250 and 3000 s/mm^2. In addition, a non-diffusion weighted measurement was acquired. Other imaging parameters included: repetition time = 2800 msec, echo time = 44 msec, matrix = 64 × 64, 5 slices, bandwidth = 7815 Hz/pixel. The *in vivo* experiment was performed on a surface rat coil using the same imaging parameters, except for 20 slices and bandwidth of 1445 Hz/pixel.

Different voxel sizes were achieved from the combination of various slice thickness and field of view with minimal image blurring. The voxel size varied between 1.210 and 2.366 mm^3 in phantom and 0.200–0.303 mm^3 in rat brains. Multiple averages were used to control SNR. Because SNR is unit free, the voxel with a median volume (1.694 mm^3) was used as a baseline for comparison. All the measured SNR in acquisition was calculated as percentage relative to this

baseline, which varied within 11% in phantom and 5% in rat. Therefore we concluded that the SNR is controlled. [Table 1] summarized the imaging parameters. [Fig. 1] showed the diffusion images from the phantom and the rat, respectively (Phantom: panel A: non-diffusion weighting; B: 750 s/mm^2 and C: 1500 s/mm^2; Rat: panel D/G: mean diffusivity/kurtosis; E/H: axial diffusivity/kurtosis; F/I: radial diffusivity/kurtosis). Different contrast between fat and water can be noticed in the phantom.

Images processing and selection of region of interest

All image processing was performed with MATLAB 7.8 (Mathworks, Natick, Mass, USA). Both the diffusion tensor and the diffusion kurtosis tensor were calculated from a series of diffusion weighted images using the diffusion kurtosis estimator [18]. In phantom analysis, the regions of interest were selected manually from the central three consecutive slices on the diffusion weighted images of b-value of 750 s/mm^2, because of the improved contrast between water and fat (seen as in [Fig. 1]). The mean value was calculated from a fixed region with a size of 200 pixels within each component of interest. Both the axial and radial kurtosis followed the definition by Jensen et al. [15]. Because the apparent diffusion coefficient of fat is too small [17], the fat component was not included in the analysis. In the rat experiment, the whole brain on the non-diffusion weighted images was selected manually. The indices of interest included the mean/axial/radial diffusivity and the corresponding diffusion kurtosis.

The SNR of the individual measurement was calculated from a non-diffusion weighted image. The signal was selected from a region of interest located either within the cream component of the phantom or from the whole brain in the rat. The noise was calculated as the standard deviation from a ghost-free region in the background.

Table 1 The imaging parameters.

voxel size (%)	voxel size (mm^3)	FOV (mm)	slice thickness (mm)	NEX	SNR (%)
phantom					
139.7	2.366	83.2	1.4	1	100.8
119.7	2.028	83.2	1.2	1	92.1
119.0	2.016	76.8	1.4	1	89.0
102.0	1.728	76.8	1.2	2	104.5
100.0	1.694	70.4	1.4	2	100.0
99.8	1.690	83.2	1.0	2	106.5
85.7	1.452	70.4	1.2	2	92.4
85.0	1.440	76.8	1.0	2	94.1
71.4	1.210	70.4	1.0	3	96.2
rat brain					
124.7	0.303	35.2	1.0	2	101.8
118.5	0.288	38.4	0.8	2	96.8
102.9	0.250	32.0	1.0	3	102.9
100	0.243	28.8	1.2	3	100.0
99.6	0.242	35.2	0.8	3	99.6
83.5	0.203	28.8	1.0	4	96.5
82.3	0.200	32.0	0.8	4	95.0

Table 1 summarized the imaging parameters used in the experiment. The voxel size was expressed in the unit of mm^3. A voxel size of 1.694 mm^3 in phantom and 0.243 mm^3 in the rat brain was used as the basis for comparison. Combination of different voxel sizes was expressed as percentage relative to the voxel size in the baseline. Multiple acquisitions were averaged in order to maintain a fixed SNR relative to the SNR in the baseline image. The SNRs in each combinations were measured from the averaged image and normalized to the SNR in the baseline image, expressed in percentage. Abbreviations used: FOV: field of view; NEX: number of excitation.

Statistical analysis

All statistical analyses were performed by using SPSS (software package for Windows version 12.0, SPSS, Chicago, IL, USA). The reproducibility analysis followed Padhani et al. [19]. Bland-Altman plots [20,21] were generated by using MedCalc for Windows, version 12.5.0 (MedCalc Software, Mariakerke, Belgium). All statistical tests were performed at the five percent level of significance.

For each measurement, the Shapiro–Wilk test was used to assess normal distribution of the samples. The squared root of the mean squared difference (dSD) and within-subject standard deviation (wSD = dSD/$\sqrt{2}$) was calculated. The repeatability was assessed by a threshold below which the absolute difference between measurements is expected to lie for 95% of pairs of observations, which is 2.77*wSD. To quantify the measurement error relative to the diffusion indices, the within-subject coefficient of variation (wCV) was calculated by dividing wSD by the global mean.

The variance ratio was calculated to compare the between-subject variance and within-subject variance for each index. A parameter with a large between-subject variance, but a small within-subject variance would have a higher value in this ratio.

Results

[Fig. 2] showed the effect of voxel size on the mean diffusivity and the mean diffusion kurtosis, which indicated that the measured values are stable throughout the range. The averaged mean diffusivity of phantom is $1.42 \pm 0.00 * 10^{-3}$ mm^2/s in water (panel A), $1.29 \pm 0.00 * 10^{-3}$ mm^2/s in cream (panel B) and $0.84 \pm 0.03 * 10^{-3}$ mm^2/s in rat (panel C). The corresponding mean diffusion kurtosis is 0.23 ± 0.01 (panel D), 0.68 ± 0.00 (panel E) and 0.82 ± 0.03 (panel F), respectively.

The Bland-Altman plots indicated the measurements of all diffusion indices are reproducible in phantom [Fig. 3: water; Fig. 4: cream] and in rat brain [Fig. 5]. The dash line indicated the 95% limit of agreement, which is approximately of 10% difference in both water and rat brains, but 5% in cream. The reproducibility is valid for the measurement of both diffusion kurtosis and diffusivity and in mean (panel A in the respective figures), axial (panel B in the respective figures) and radial (panel C in the respective figures) directions.

For between-scans reproducibility analysis, the Shapiro–Wilk test indicated a normal distribution for all measurements ($p > 0.05$). The mean value of measurements, within-subject standard deviations, repeatability, within-subject coefficient of variation and variance ratio were summarized for phantom [Table 2] and rat brains [Table 3],

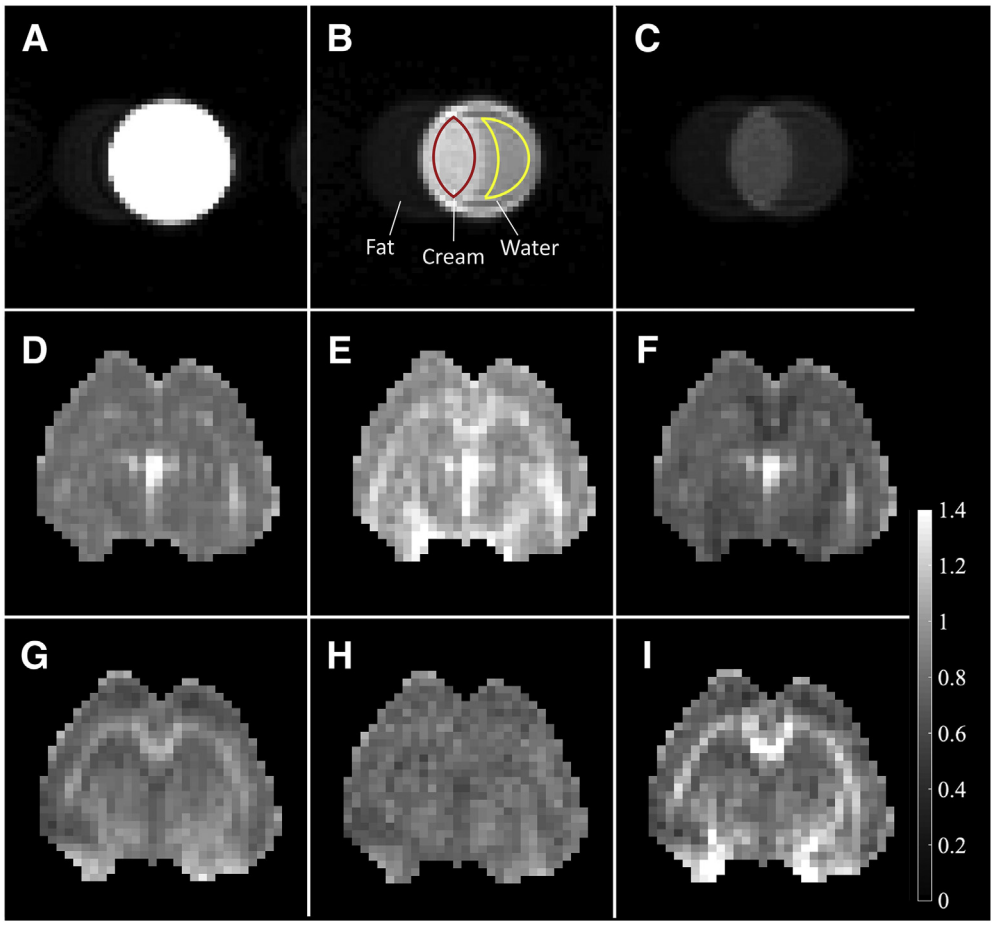

Fig. 1 Diffusion weighted images. The diffusion images in the phantom showed the differentially enhanced contrast between fat and water with b value of (A) 0 s/mm^2, (B) 750 s/mm^2 and (C) 1500 s/mm^2. The *in vivo* images from one representative slice of the rat showed the mean (D), axial (E) and radial (F) diffusivities and the corresponding kurtosis (G–I).

respectively. In the phantom experiment, the within-subject coefficient of variation was less than 6.99%. The measurement of mean diffusivity is relatively stable (ranged between 0.88 and 1.69% in water; 0.88–1.05% in cream) when compared to the corresponding mean diffusion kurtosis (ranged between 1.66 and 6.99% in water; 1.03–3.09% in cream). In addition, variation in cream is generally smaller than water (ranged between 0.88 and 3.09%), in term of both mean diffusivity and mean diffusion kurtosis.

The variance ratio demonstrated good stability in all measurements (all $p > 0.05$), except for two at border (the mean diffusion kurtosis of water at voxel size of 1.452 mm^3, $p = 0.048$ and 1.694 mm^3, $p = 0.033$). Increased variance ratio can be noticed in most of the measurements of kurtosis of water (larger than 1) rather than cream, which might suggest increased fluctuation in water among the different voxel sizes.

Discussion

The effect of spatial resolution on the diffusion MRI measurement was assessed using a range of voxel size that is close to the general practice of the rat brain between 0.200 and 0.303 mm^3 and when the SNR remained controlled. The within subject variations and repeatability analysis showed good consistency in all measurements using a phantom of two compartments and from the rat brain. The study provides a reference value for quality control and evidence of reliability for comparisons between studies.

The reproducibility of the diffusion measurement

Diffusion measurement could be over or under-estimated when using different voxel sizes, which was related to the noise level. As the SNR decreased, the largest eigenvalue would be over-estimated; the smallest eigenvalue would be under-estimated [16]. This observation is valid under Gaussian diffusion. However, the effect of voxel size on the diffusion measurement might be different when under a condition of multiple compartments where the diffusion is deviated from Gaussianity. Diffusion imaging in human brain showed that increasing voxel size could bias mean, axial and radial diffusivities to higher values [22].

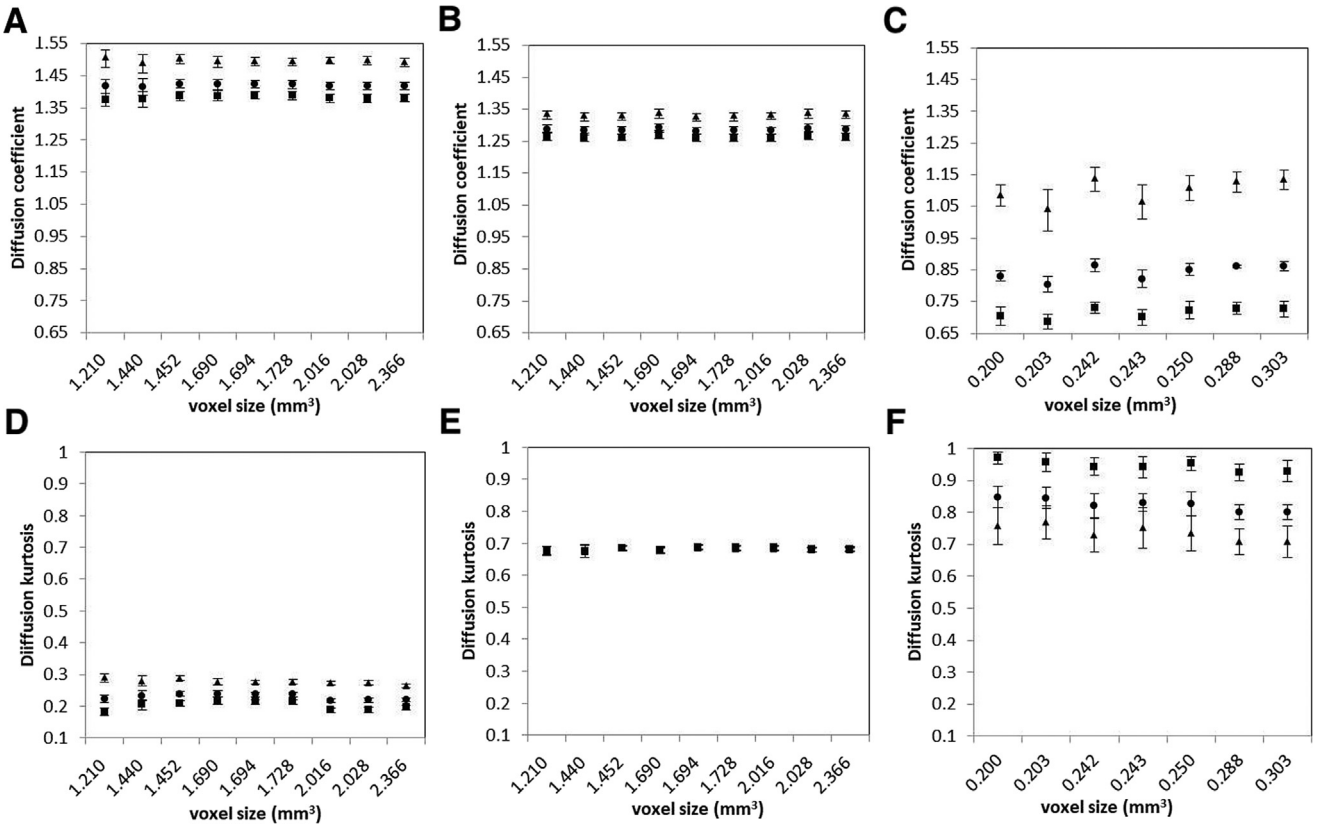

Fig. 2 The effect of the voxel size on the diffusion index. The figure showed the effect of voxel size on the measurement of diffusion index in water (A,D), cream (B,E) and rat (C,F), respectively. The top row plotted the measurement for diffusivity and the bottom for kurtosis. The triangle indicated axial diffusivity/kurtosis; square: radial; circle: mean. The voxel size is in unit of mm^3. All diffusivities are measured in units of 10^{-3} mm^2/sec. Diffusion kurtosis is dimensionless.

In the current study, the reproducibility was examined between two cream phantoms and two rats, with each repeated for 3 times. The diffusion measurement is reproducible within the range of the voxel sizes in investigation, in terms of the following 3 aspects: A. under different conditions, i.e. single compartment (water), two compartments (cream) and the *in vivo* environment (rat brain); B. among diffusion amplitude (diffusivity) and distributions (diffusion kurtosis) and C. along axial, radial and averaged in all directions. This can be evident from the within-subject coefficient of variation, which is 0.88%–6.99% for phantom and 0.69%–6.19% for the rat brain.

In the cream phantoms, 2 outliers were noticed [Figs. 3 and 4]. Both are results from the first two measurements, probably due to fluctuation in the scanner performance. Otherwise, the statistics [Tables 2 and 3] demonstrated low variation among the phantom and the rat measurements. It is therefore suggested that the diffusion imaging is stable in a multi-compartment model.

In the phantom measurements, the result from the two-compartment component (cream) showed improved performance than in single compartment (water), in term of fluctuation between different voxel sizes, repeatability and variance ratio. This observation might be related to the difference in diffusion properties under the compartmental environment. When compared to the phantom, the *in vivo* experiment showed increased variation in these indices, probably due to physiological motion. However, all deviations in the study are within the 95% of agreement.

The current study demonstrated that the diffusion parameters, such as mean diffusivity and diffusion kurtosis, are reproducible and repeatable in a two compartment phantom and in biological environment if at the similar level of SNR. This finding supports the previous hypothesis that the main factor contributing to the deviation in diffusion measurement could be related to noise.

Reproducibility in phantom and in vivo

A range of phantoms are available in studies related to measurement of diffusivity or diffusion kurtosis. These phantoms mainly belonged to the following two categories: homogeneous therefore isotropic; heterogeneous and anisotropic. However, in a scenario of multi-compartments, the diffusion could be heterogeneous and isotropic. The cream phantom provided an environment that is isotropic and consisted of two compartments.

The mean kurtosis in either the water or cream component of our two compartment phantom are significantly higher than measured from water in a single compartment phantom [23]. Different interaction between the water component and the fat globules might exist. The study therefore provided evaluation in a setting that is close to the realistic

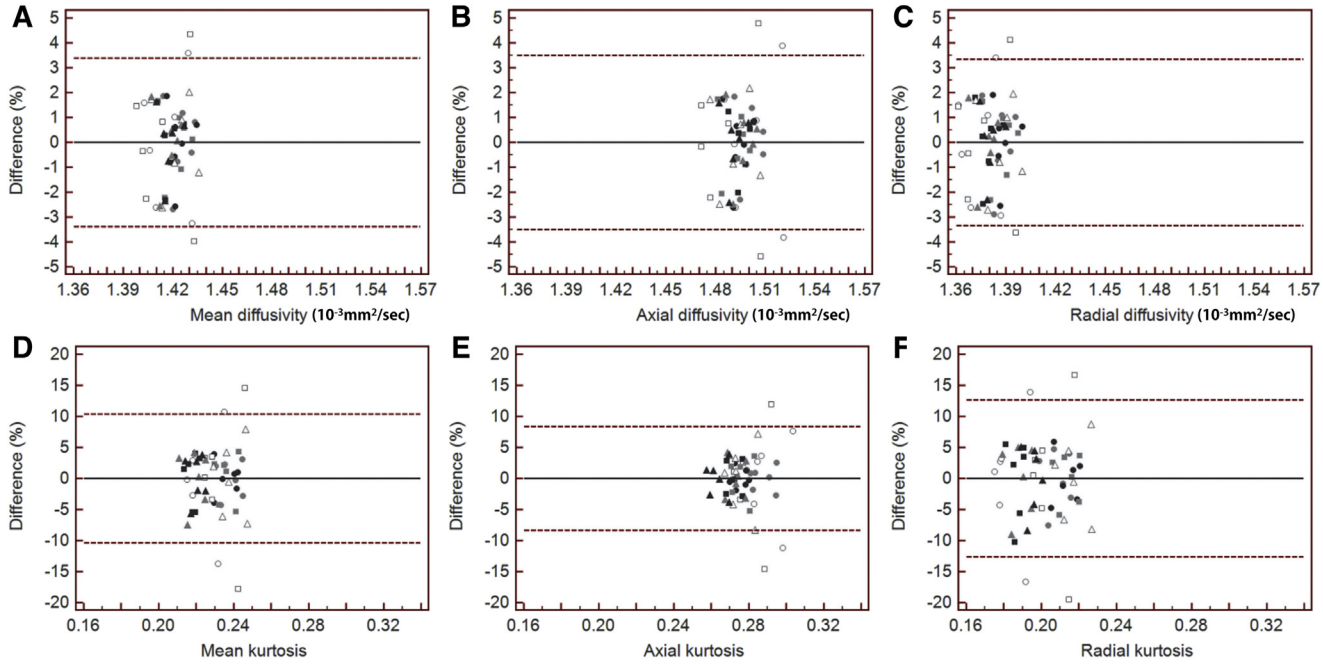

Fig. 3 Reproducibility of diffusion measurement in water. The figure showed Bland-Altman plots from the water component of the phantoms, each repeated 3 times. The diffusivity in water included (A) mean, (B) axial and (C) radial. The corresponding diffusion kurtosis was shown in panel (D), (E) and (F), respectively. All diffusion coefficients are in units of 10^{-3} mm^2/s. The diffusion kurtosis is dimensionless. The dash line indicated the 95% limit of agreement. Different markers indicated different field of view (circle: 70.4 mm, square: 76.8 mm and triangle: 83.2 mm) and slice thickness (blank: 1.0 mm, shaded: 1.2 mm and solid: 1.4 mm).

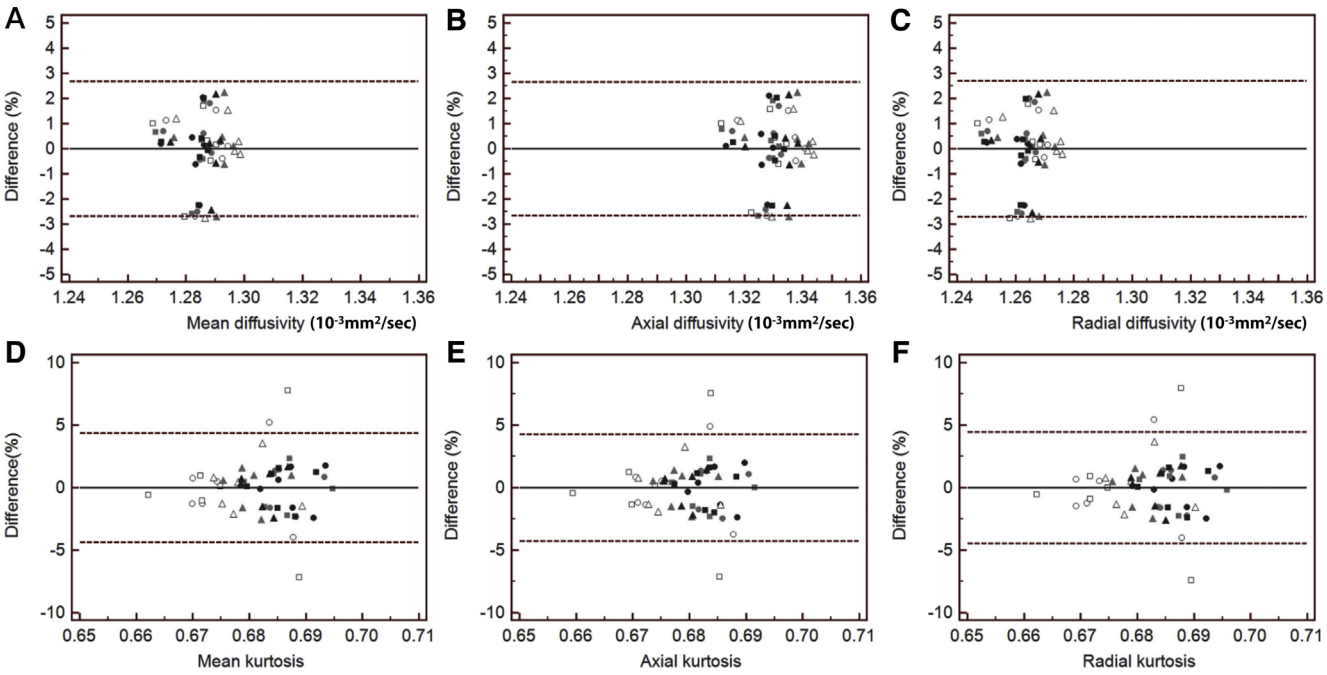

Fig. 4 Reproducibility of diffusion measurement in cream. The figure showed Bland-Altman plots from the cream component of the phantoms, each repeated 3 times. The diffusivity in cream included (A) mean, (B) axial and (C) radial. The corresponding diffusion kurtosis was shown in panel (D), (E) and (F), respectively. All diffusion coefficients are in units of 10^{-3} mm^2/s. The diffusion kurtosis is dimensionless. The dash line indicated the 95% limit of agreement. Different markers indicated different field of view (circle: 70.4 mm, square: 76.8 mm and triangle: 83.2 mm) and slice thickness (blank: 1.0 mm, shaded: 1.2 mm and solid: 1.4 mm).

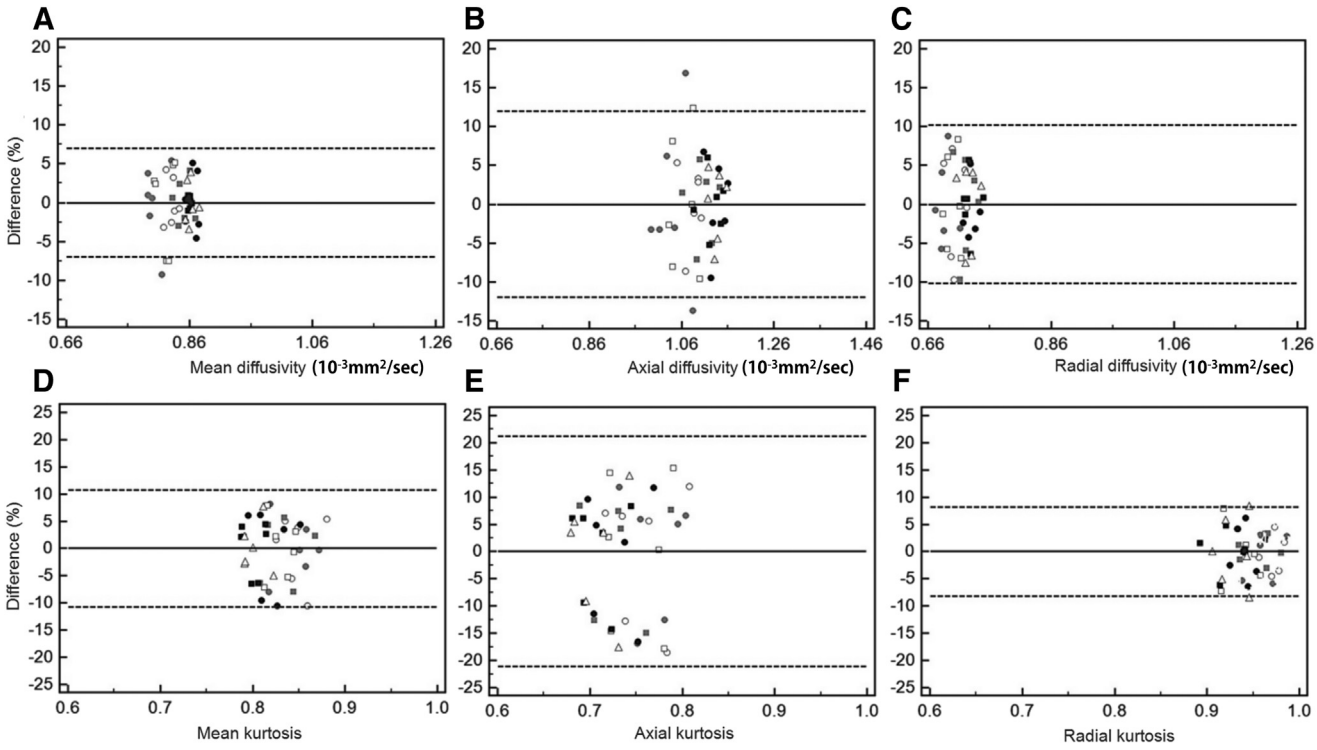

Fig. 5 Reproducibility of diffusion measurement in rat. The figure showed Bland-Altman plots from the *in vivo* experiment. The diffusivity from the rats included (A) mean, (B) axial and (C) radial. The corresponding diffusion kurtosis was shown in panel (D), (E) and (F), respectively. All diffusion coefficients are in units of 10^{-3} mm^2/s. The diffusion kurtosis is dimensionless. The dash line indicated the 95% limit of agreement. Different markers indicated different field of view (circle: 32.0 mm, square: 28.8 mm, triangle: 35.2 mm and star: 38.4 mm) and slice thickness (blank: 0.8 mm, shaded: 1.0 mm and solid: 1.2 mm).

Table 2 Reproducibility statistics in phantom.

Voxel size (mm^3)/(%)	1.210/71.4	1.440/85.0	1.452/85.7	1.690/99.8	1.694/100.0	1.728/102.0	2.016/119.0	2.028/119.7	2.366/139.7
Global mean									
MD_w	1.41 ± 0.02	1.41 ± 0.02	1.42 ± 0.01	1.42 ± 0.01	1.42 ± 0.01	1.42 ± 0.01	1.41 ± 0.01	1.41 ± 0.01	1.41 ± 0.01
MD_c	1.28 ± 0.01	1.28 ± 0.01	1.28 ± 0.01	1.29 ± 0.01	1.28 ± 0.01	1.28 ± 0.01	1.28 ± 0.01	1.29 ± 0.01	1.28 ± 0.01
MK_w	0.22 ± 0.01	0.23 ± 0.01	0.23 ± 0.00	0.23 ± 0.01	0.23 ± 0.00	0.23 ± 0.00	0.21 ± 0.00	0.21 ± 0.00	0.22 ± 0.00
MK_c	0.67 ± 0.01	0.67 ± 0.01	0.68 ± 0.00	0.67 ± 0.00	0.68 ± 0.00	0.68 ± 0.00	0.68 ± 0.00	0.68 ± 0.00	0.68 ± 0.00
Within subject standard deviation (*10^{-2})									
MD_w	2.39	2.69	1.51	1.68	1.37	1.31	1.26	1.35	1.26
MD_c	1.23	1.25	1.21	1.27	1.17	1.23	1.14	1.35	1.25
MK_w	1.22	1.67	0.46	0.92	0.39	0.6	0.61	0.64	0.53
MK_c	1.36	2.12	0.71	0.91	0.76	0.74	0.72	0.73	0.71
Repeatability (*10^{-2}) ($\alpha = 0.05$)									
MD_w	6.62	7.46	4.18	4.67	3.8	3.62	3.48	3.73	3.48
MD_c	3.42	3.47	3.35	3.51	3.23	3.42	3.16	3.74	3.46
MK_w	3.37	4.61	1.27	2.56	1.09	1.66	1.69	1.78	1.46
MK_c	3.76	5.88	1.96	2.52	2.11	2.06	1.99	2.03	1.96
Within subject coefficient of variation (%)									
MD_w	1.69	1.89	1.06	1.19	0.96	0.92	0.88	0.95	0.89
MD_c	0.96	0.98	0.94	0.99	0.91	0.96	0.88	1.05	0.97
MK_w	5.46	6.99	1.94	3.97	1.66	2.75	2.56	2.93	2.39
MK_c	2.01	3.09	1.03	1.35	1.11	1.09	1.06	1.08	1.04
Variance ratio									
MD_w	0.32	0.57	0.11	0.97	0.01	0.75	0.01	0.25	0.00
MD_c	1.13	1.10	0.27	1.33	0.11	0.49	0.31	0.46	0.30
MK_w	1.33	0.61	7.94[a]	1.97	10.13[b]	2.51	0.20	2.74	1.91
MK_c	0.57	0.15	1.26	0.96	0.48	1.51	0.63	0.53	0.09

It summarized the reproducibility analysis of diffusion index under different voxel sizes in the phantom. The statistics included within-subject variation, repeatability, within-subject coefficient of variation and variance ratio. Abbreviations used: MK_w: mean diffusion kurtosis of water; MK_c: mean diffusion kurtosis of cream; MD_w: mean diffusivity of water; MD_c: mean diffusivity of cream.

Table 3 Reproducibility statistics for *in vivo* experiment.

Voxel size (mm^3)/(%)	0.200/82.3	0.203/83.5	0.242/99.6	0.243/100	0.250/102.9	0.288/118.5	0.303/124.7
Global mean							
MD	0.83 ± 0.02	0.80 ± 0.03	0.87 ± 0.02	0.82 ± 0.03	0.85 ± 0.02	0.86 ± 0.00	0.86 ± 0.02
MK	0.85 ± 0.04	0.84 ± 0.03	0.82 ± 0.04	0.83 ± 0.02	0.82 ± 0.03	0.80 ± 0.02	0.80 ± 0.02
Within subject standard deviation ($*10^{-2}$)							
MD	2.09	3.69	2.79	3.8	2.33	0.60	2.11
MK	4.85	3.87	5.08	3.29	4.00	3.01	2.61
Repeatability ($*10^{-2}$) ($\alpha = 0.05$)							
MD	5.79	10.22	7.73	10.53	6.46	1.65	5.84
MK	13.44	10.71	14.06	9.10	11.09	8.35	7.24
Within subject coefficient of variation (%)							
MD	2.53	4.59	3.23	4.64	2.73	0.69	2.46
MK	5.71	4.60	6.19	3.98	4.89	3.77	3.27
Variance ratio							
MD	1.93	0.63	0.00	0.08	1.51	1.16	1.86
MK	0.63	1.12	0.19	0.01	1.47	0.00	0.42

It summarized the reproducibility analysis of diffusion index under different voxel sizes for the *in vivo* experiment. The statistics included within-subject variation, repeatability, and within-subject coefficient of variation and variance ratio. Abbreviations used: MK: mean diffusion kurtosis; MD: mean diffusivity.

heterogeneous condition. Noticeably, the diffusion kurtosis in the rat is consistent with literature [15].

Compared with the cream phantom, the mean diffusivity in rat is reduced and the mean diffusion kurtosis increased. This observation might be related to the hindered or restricted diffusion in the biological environment, the contamination from physiological motion, or both. Increased variation in the *in vivo* measurements was noticed, but the reproducibility and repeatability are within the 95% confidence level. The result demonstrated a good stability and reproducibility of diffusion measurement even under a complicated compartmental diffusion and with motion artifact. The study might increase the confidence of the use of both DTI and DKI in the routine practice or animal experiment.

Limitation

Because of the repeated measurements, the cream was kept in the scanner room for 14 h. The main limitations in the study is the potential degradation of the cream phantom. Furthermore, the two compartment model often assumed the same T2 relaxation in both fat and water, which is indeed different. The heating procedure has been proposed to minimize such difference. The current study did not heat up the cream phantom because it might result in potentially different water concentration between phantoms during the process. Even though the reproducibility can be affected by these limitations, the variation is still minimal.

Conclusion

The measurement of diffusion in an isotropic and heterogeneous phantom as well as the rat brain is consistent with different spatial resolutions when controlled SNR, and reproducible for repeated measurements.

Conflicts of interest

All authors have no actual or potential conflicts of interest to disclose.

Funding

This work was financially supported by the Ministry of Science and Technology Taiwan (grant MOST 106-2314-B-182 -018 -MY3, MOST 106-2911-I-182-505, MOST 107-2911-I-182-503), the Healthy Aging Research Center of Chang Gung University (grant EMRPD1H0411, EMRPD1H0551, EMRPD1H0431, EMRPD1I0501, EMRPD1I0471), and the Chang Gung Memorial Hospital (grants CMRPD1G0561-2, and CMRPG2B0251).

Acknowledgments

This work was supported by Healthy Aging Research Center, Chang Gung University, Taiwan. The imaging facility was supported by Center for Advanced Molecular Imaging and Translation, Chang Gung Memorial Hospital, Taiwan. The funding source had no involvement in the collection, analysis and interpretation data; in the writing of the report; and in the decision to submit the paper for publication. The author would like to acknowledge the contribution from Dr. YauYau Wai from Department of Radiology, Chang Gung Memorial Hospital, Keelung, who unfortunately passed away before the manuscript is accepted.

REFERENCES

[1] Le Bihan D, Breton E, Lallemand D, Aubin ML, Vignaud J, Laval-Jeantet M. Separation of diffusion and perfusion in intravoxel incoherent motion MR imaging. Radiology 1988;168:497–505.

[2] Turner R, Le Bihan D, Maier J, Vavrek R, Hedges LK, Pekar J. Echo-planar imaging of intravoxel incoherent motion. Radiology 1990;177:407–14.

[3] Yamada I, Aung W, Himeno Y, Nakagawa T, Shibuya H. Diffusion coefficients in abdominal organs and hepatic lesions: evaluation with intravoxel incoherent motion echo-planar MR imaging. Radiology 1999;210:617–23.

[4] Moseley ME, Cohen Y, Kucharczyk J, Mintorovitch J, Asgari HS, Wendland MF, et al. Diffusion-weighted MR imaging of anisotropic water diffusion in cat central nervous system. Radiology 1990;176:439–45.

[5] Basser PJ, Mattiello J, LeBihan D. Estimation of the effective self-diffusion tensor from the NMR spin echo. J Magn Reson B 1994;103:247–54.

[6] Basser PJ, Mattiello J, LeBihan D. MR diffusion tensor spectroscopy and imaging. Biophys J 1994;66:259–67.

[7] Pfefferbaum A, Sullivan EV, Hedehus M, Lim KO, Adalsteinsson E, Moseley M. Age-related decline in brain white matter anisotropy measured with spatially corrected echo-planar diffusion tensor imaging. Magn Reson Med 2000;44:259–68.

[8] Wang J, Wai Y, Lin WY, Ng S, Wang CH, Hsieh R, et al. Microstructural changes in patients with progressive supranuclear palsy: a diffusion tensor imaging study. J Magn Reson Imaging 2010;32:69–75.

[9] Wang JJ, Lin WY, Lu CS, Weng YH, Ng SH, Wang CH, et al. Parkinson disease: diagnostic utility of diffusion kurtosis imaging. Radiology 2011;261:210–7.

[10] Basser PJ, Pajevic S, Pierpaoli C, Duda J, Aldroubi A. In vivo fiber tractography using DT-MRI data. Magn Reson Med 2000;44:625–32.

[11] Conturo TE, Lori NF, Cull TS, Akbudak E, Snyder AZ, Shimony JS, et al. Tracking neuronal fiber pathways in the living human brain. Proc Natl Acad Sci U S A 1999;96:10422–7.

[12] Stejskal EO, Tanner JE. Spin diffusion measurements: spin echoes in the presence of a time-dependent field gradient. J Chem Phys 1965;42:288–92.

[13] Jensen JH, Helpern JA, Ramani A, Lu H, Kaczynski K. Diffusional kurtosis imaging: the quantification of non-Gaussian water diffusion by means of magnetic resonance imaging. Magn Reson Med 2005;53:1432–40.

[14] Lu H, Jensen JH, Ramani A, Helpern JA. Three-dimensional characterization of non-Gaussian water diffusion in humans using diffusion kurtosis imaging. NMR Biomed 2006;19:236–47.

[15] Jensen JH, Helpern JA. MRI quantification of non-Gaussian water diffusion by kurtosis analysis. NMR Biomed 2010;23:698–710.

[16] Bastin ME, Armitage PA, Marshall I. A theoretical study of the effect of experimental noise on the measurement of anisotropy in diffusion imaging. Magn Reson Imag 1998;16:773–85.

[17] Fieremans E, Pires A, Jensen JH. A simple isotropic phantom for diffusional kurtosis imaging. Magn Reson Med 2012;68:537–42.

[18] Tabesh A, Jensen JH, Ardekani BA, Helpern JA. Estimation of tensors and tensor-derived measures in diffusional kurtosis imaging. Magn Reson Med 2011;65:823–36.

[19] Padhani AR, Hayes C, Landau S, Leach MO. Reproducibility of quantitative dynamic MRI of normal human tissues. NMR Biomed 2002;15:143–53.

[20] Bland JM, Altman DG. Measuring agreement in method comparison studies. Stat Methods Med Res 1999;8:135–60.

[21] Bland JM, Altman DG. Statistics Notes: measurement error and correlation coefficients. BMJ 1996;313:41–2.

[22] Papinutto ND, Maule F, Jovicich J. Reproducibility and biases in high field brain diffusion MRI: an evaluation of acquisition and analysis variables. Magn Reson Imaging 2013;31:827–39.

[23] Jansen JF, Stambuk HE, Koutcher JA, Shukla-Dave A. Non-Gaussian analysis of diffusion-weighted MR imaging in head and neck squamous cell carcinoma: a feasibility study. AJNR. Am J Neuroradiol 2010;31:741–8.